Journal of Climate Change, Vol. 7, No. 2 (2021), pp. 63-72.
DOI 10.3233/JCC210012

Surface Reflectance Change can Induce Reduction in the Surrounding Ambient Environment Warming

Bikram Sen Sahu[1,2]*, Pyarimohan Maharana[2], Ankit Tandon[3] and Arun K. Attri[2]

[1]Department of Natural Resources Management and Geoinformatics, Khallikote University, Konisi Berhampur - 761008, India
[2]School of Environmental Sciences, Jawaharlal Nehru University, New Delhi - 110067, India
[3]School of Earth and Environmental Sciences, Central University of Himachal Pradesh Dharamshala, Kangra - 176215, India
✉ bssahu@khallikoteuniversity.ac.in

Received September 4, 2020; revised and accepted May 18, 2021

Abstract: Global warming has emerged as a major issue of concern as the fallout would have a wide-spread impact on many climate processes in addition to posing a serious threat for human development, directly or in-directly. COP21 at the Paris agreement settled to limit global warming well below 2°C in the future. This goal can be attained by ensuring a drastic reduction in the emission of greenhouse gases or by cutting down the use of energy consumption, an obvious solution but difficult to implement. A more acceptable and easy approach would be to reduce the use of energy to cool buildings and surfaces by adopting simple scientific techniques. The present work explores the feasibility of one such approach, which can be applied in large cities and urban regions; knowing that by increasing the surface reflectance (albedo) for incoming solar short wave (SSW) radiation it is possible to decrease the temperature of the surface. If the appropriated surface area is large enough then it is possible to cause a decrease in the ambient air temperature. Three different types of heat-resistant Superseal Thermoflex P-111 coatings of different colours were applied on the roof surface to evaluate their respective reflectance properties towards the incoming SSW radiation incident on the roof with reference to the resulting surface temperature. The average reflectance in the spectral range 280-880 nm – for dark pink, light pink and white colour coats – were estimated as 0.44, 0.61 and 0.76, respectively; the obtained values were significantly larger than that observed for asphalt/cement coated surfaces. The higher reflectance of white coating leads to less heat absorption by the roof surface open to the SSW radiation and thus a significant drop in the surface temperature. Also, the heat transmitted underneath the surface space will be much reduced, even the emission (loss) of radiation (Infra-Red) from such a surface into the surrounding environment will be reduced.

Keywords: Global warning; Reflectance; Energy conservation; Energy spectra; Albedo.

Introduction

In the present era, global warming has arisen as an issue of concern that has serious implications for the biosphere and human population; direct or indirect (James et al., 2017; Hossain et al., 2016). The Paris agreement (2015) in the 21st Conference of Parties (COP21) of the United Nations Framework Convention on Climate Change (UNFCCC, 2015) suggested options combat the global temperature rise (Rayner Tim et al., 2019). All parties agreed to counter the global warming by keeping the rise in the average global ambient temperature well below 2°C in the future; even this rise causes serious concern for many vulnerable nations

*Corresponding Author

(island nations and countries having vast coastlines) and poses a threat to their existence from the anticipated sea-level rise. The vulnerable nations advocate the global temperature rise within 1.5 °C, which may reduce the effect of climate change (Sellers et al., 1996; UNFCCC, 2015; Chen et al., 2017; James et al., 2017). To achieve the set limits for the global rise in the ambient temperature, and avert the ensued widespread effects on the Earth's physical environment, it is important that all the stake holders such as the scientists, engineers, policy makers, politicians, and citizens must work in concert. The major concerns arising from the increase in the average global temperature are a disruption in the hydrological cycle, glacier melting, increase in sea level, excess/deficit rainfall, a threat to food security, and the enforced changes on human demography (Pachauri et al., 2014; Fischer and Knutti, 2015; Arnell et al., 2016; Schleussner et al., 2016; Kraaijenbrink et al., 2017; Mohammed et al., 2017; Vautard et al., 2014; Karmalkar and Bradley, 2017; Xu et al., 2017). In view of the anticipated widespread disruption of the existing natural environment's attributes and the induced multifarious adverse impact on the man-centric developmental aspects, it is but imperative to seek scientific rational solutions to curtail the rising global warming trend. In this note, we outline a simple and benign solution based on the physics of the surface reflectance properties to arrest the warming trend.

The most discussed option, in this regard, is by directly controlling the increase in the concentrations of greenhouse gases in the atmosphere or by reducing the use of energy at the local, regional and global levels (Cui et al., 2009; Jacobson and Ten Hoeved, 2012); this is, but complicated and tedious to implement and has resulted in only partial success. It is difficult to compromise on the respective national economic development goals by capping or reducing the use of energy, particularly as the rising human population (≥7 billion) pushes the energy consumption demand upwards (Caldeira and Brown, 2019). However, approaches using the established principles of physics to decrease the ambient temperature or energy use are more feasible as they do not require a compromise at the level of economic development (Allen et al., 1969; Rosenfield et al., 1998; Jacobson and Hoeved, 2012; Gaffin et al., 2012). The current trends of using electricity-based cooling devices (air-conditioners) in urban areas during summer and for heating during winter have further added to global warming (IPCC, 2015). Any benign but science-based measure would have a significant impact in not only lowering the use of energy to cool or heat the human dwellings but also have the corresponding impact to cause a decline in CO_2 release into the atmosphere (Jahandideh-Tehrani et al., 2015; Bartos and Chester, 2015; Kraucunas et al., 2015; van Vliet et al., 2016; Arnfield, 2003; Weng et al., 2004; Shunlin et al., 1998; Tadeu et al., 2005). Due to the absorption and holding capacity of heat, an urban area experiences a much warmer temperature than the nearby rural area. This phenomenon is known as Urban Heat Island (UHL) (Oke, 1982). UHL impacts the local weather condition of a region (Rizwan et al., 2008; Myrup, 1969). The approach presented in this note exploits the consequence of the interaction of different colour coated surfaces with the incoming solar short wave (SSW) radiation in terms of their reflectance. If the major part of the incident SSW radiation can be reflected back into space and knowing that the Earth's atmosphere is transparent towards SSW, it stands to reason that the absorption of SSW incident on surfaces will significantly decrease. If this decrease is significant and the surface area is large enough then the surface will cool significantly, and this would contribute toward decreasing the temperature of the atmosphere in contact. In this regard, it is important to state that a significantly large roof surface area can be appropriate for the houses and large buildings in urban areas.

Interaction of Solar Radiation in the Atmosphere

Essentially, the solar radiation entering the Earth's atmosphere is designated as SSW and comprises of a small fraction of ultraviolet (200-400 nm), predominant part as visible radiation (400-700 nm) and infra-red radiation (>700 nm) (Myers et al., 2004; Blonquist and Bugbee, 2018; Denning, 2018). Through its passage towards Earth's surface, most of the ultraviolet fraction is filtered out or absorbed (Stratospheric Ozone layer) and a small part of the SSW undergoes reflection involving Earth's atmospheric constituents (Figure 1). SSW energy received at the top of the atmosphere mostly resides in the visible spectrum and the constituents of the atmosphere are essentially transparent (no absorption) to the visible radiation fraction (Jacquemoud and Baret, 1990; Goodin et al., 1993; Jacquemoud et al., 1995; Jacquemoud et al.,1996). The composition of total solar spectrum energy in different distinctive parts at the top of the atmosphere and on the Earth's surface is analysed using the ASTM G173-03 reference spectra developed by the North American PV industry and the American Society for Testing and Materials (ASTM)

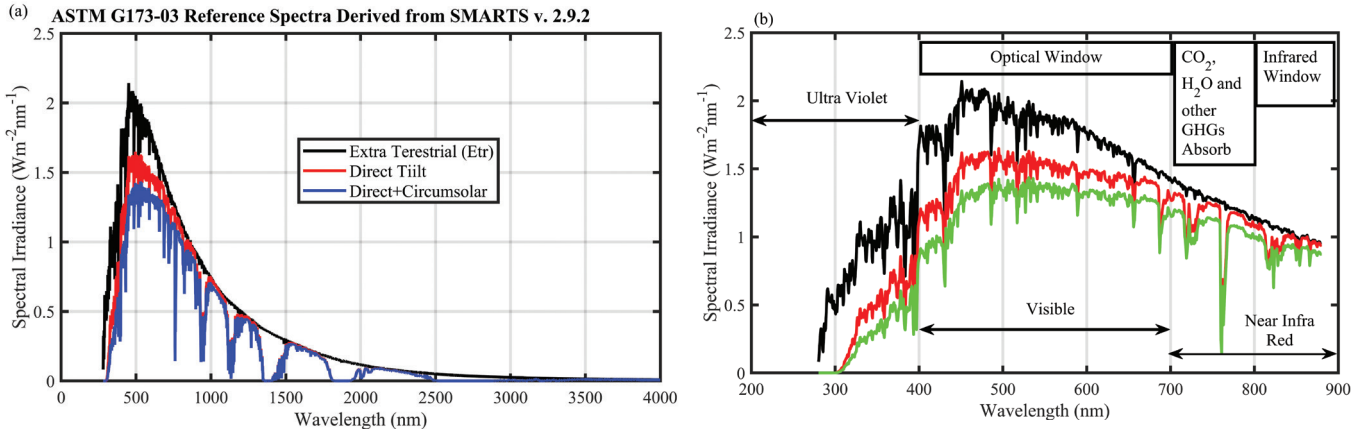

Figure 1: (a) ASTM G173-03 Reference Spectra Derived from SMARTS v.2.9.2 showing the average total solar radiation received outside the atmosphere of the earth (black curve), on different surface orientations (red curve, direct tilt), direct + circumsolar (blue) and (b) Solar spectral spread received on the ground. (The information is available in American Society for Testing and Materials, 2012; NREL, 2015.).

(Figure 1a,b; ASTM, 2012; NREL, 2015). The standard spectra are measured for direct normal and global tilted (at 37º) spectral irradiance and have been used in many earlier studies (Marzo et al., 2018, 1996; Simpson and Mcpherson, 1997; Jacquemoud et al., 2000; Denning, 2018). The average distribution of energy in percentage for different spectral components is given in Table 1. Most of the UV component of solar irradiance is filtered out in the stratosphere by the stratospheric photochemical reaction involving ozone and a small fraction of UV reaches the ground in the spectral range 280-400nm (Sahu et al., 2017). Of the total solar energy reaching the ground, on an average, the fractions in UV, visible and IR spectral regions are 8%, 40% and 52% (Dennings, 2018; Henderson, 1992; Ben-Dor and Banin, 1995; Islam et al., 2003; Brown et al., 2006; Small, 2006; Boyton, et al., 2007; Summers et al., 2011). The solar spectrum radiation, other than the visible spectra, while passing through the atmosphere is significantly attenuated (absorption, reflection and scattering) by the atmospheric constituents (O_3, O_2, CO_2, H_2O, aerosols, cloud, etc) before reaching the ground (Figure 1b; Blonquist and Bugbee, 2018). On the other hand, the SSW fraction's (visible light) attenuation while passing through the atmosphere is significantly less as its absorption by the constituents is absent. It follows that if a fraction of visible radiation is reflected back from the surfaces located on the Earth it will be reflected back to space without getting absorbed; whereas the radiation lying in the IR region emitted from the surfaces will be retained by CO_2, H_2O and other greenhouse gases on reflection (GHGs) (Monteith, 1970; Matthews, 1983; Mustard, 2005; Akbari et al., 2008).

Table 1: Solar spectrum energy distribution

Waveband (nm)	*Energy (%)*
0-200	0.7
200-280 (UV-C)	0.5
280-320 (UV-B)	1.5
320-400 (UV-A)	6.3
400-700 (Visible)	39.8
700-1500 (near Infra-Red)	38.8
1500-∞	12.4

Attributes of the Solar Radiation Passing through the Atmosphere and Reaching the Ground

A fraction of the incoming solar radiation passing through the atmosphere is reflected back to space on account of the average reflectance of the Earth (The Earth's albedo). On an average, about 30% of the incoming radiation is reflected back before it reaches the ground. The reflection is a function of many surface-specific characteristics and the type of incident wavelength; consequently, the reflectance varies significantly with the changes in the surface character (composition, colour, etc.): snow-covered surface reflectance may exceed 0.8 and asphalt coated surface can have this value as small as 0.1 (Sellers et al., 1986; Levinson and Akbari, 2002; Bowyer and Danson, 2004).

Incoming SSW solar radiation after passing through the Earth's atmosphere (average albedo 0.3) can be reflected/refracted/scattered or absorbed depending on the nature of the surface encountered; if the reflected fraction increases then the fraction absorbed by the surface will correspondingly decrease. The characteristic nature of reflected SSW radiation does not change and this fraction goes back to the atmosphere. However, the absorbed fraction of SSW radiation heats up the surface and raises its temperature, its loss from the surface, after its absorption, is as longwave radiation (near and far IR) and the atmosphere is not transparent to this spectral region– longwave radiation is absorbed by water vapour, CO_2 present in the atmosphere– (Stoner and Baumgardner, 1981; Malthus and Dekker, 1995; Rosenfeld et al., 1998; Islam et al., 2003). Absorbed SSW radiation transforms into heat which can either be emitted back into the atmosphere or transferred into the surface by conduction (Malthus and Dekker, 1995; Simpson and Mcpherson, 1997; Ustin et al., 1998; Jin et al., 2004; Viscarra Rossel et al., 2006). Wavelength span and the associated energy magnitude of heat radiation emitted from the surface to the atmosphere can be estimated using Stefan-Boltzmann law as given below.

$$(e_\lambda = \sigma T^4) \quad (1)$$

where e_λ represents the energy at a given wavelength λ, σ represents Stefan-Boltzmann constant and T (^{o}K) represents the temperature of the surface. It is pertinent to state that (1) surfaces having large reflection would absorb less energy, (2) less energy absorption implies lower surface temperature and the surface would emit radiation (loss) in near and far IR region, and (3) the emitted radiation in near and far IR region can be trapped by atmospheric CO_2, H_2O (vapour) and other global warming gases (GWG). The stated rationale is that when surface reflectance is high for the visible fraction of SSW, the surface not only absorbs less SSW radiation but also emit less in near and far IR radiation region into the atmosphere. Consequently, enhancing the surface reflectance in a region by appropriating large surface areas can be an effective approach to decrease global warming.

Following the above-stated rationale, systematic experiments were performed by applying different coloured polymer coatings over a cemented surface to simulate conditions similar to the one commonly encountered on the roofs of the buildings (houses and commercial buildings) in the Delhi region. The experiments were designed to measure the extent of reflection caused by the different colour coatings of surfaces with reference to incident light in the wavelength span 280-880 nm. The wavelength span conformed to the incoming SSW radiation (Figure 1). The following section details the methodology; after which the Results and Discussion section is given, while the summary of this study along with the concluding remarks is provided in section Summary and Conclusion.

Material used and Methodology

Materials used for the Experiment

Small discs made of cement (2.5cm diameter), composition similar to that is found on the roof surfaces, were coated with heat reflecting Superseal Thermoflex P-111 procured in three colours– (a) white (W), (b) light pink (LP) and (c) dark pink (DP)– from Supertech Chemicals Specialties Pvt. Ltd. (Navi Mumbai, India). The details of the product and their application procedure can be obtained from https://www.indiamart.com/supersealchem/heat-insulation-membrane-coating.html. This coating material is commercially used to seal the roof surfaces of buildings.

Methodology

The reflectance of the discs was measured using a Shimadzu UV-Visible spectrophotometer equipped with an integrated reflectance measuring accessory (integrating sphere UV-2200/24002500 series). Prior to the measurement of Superseal thermoflex coated discs, calibration was done with reference to $BaSO_4$ coated discs (100% reflectance) and black carbon-coated discs (reflectance 0%) in the spectral span ranging from 280 to 880 nm. All reflectance measurements were carried out with reference to the calibration. To ascertain the temperature of a surface under a real condition, the whole roof surface of a house at Jawaharlal Nehru University was coated with W heat reflecting Superseal Thermoflex P-111 procured from Supertech Chemicals Specialties Pvt. Ltd. (Navi Mumbai, India). The roof surface of the adjoining house had a dark asphalt coating, typically used for coating the roofs, as a reference. The experiment was done to measure the roof surface temperature by using a non-contact Infrared thermometer equipped with a built-in laser pointer capable of measuring the surface temperature with ±0.1^{o}C from a distance (MEXTECH 8858/8859 series IR Thermometer, Mextech technologies India).

Results

Reflection Profile of DP, LP and W Coated Surfaces (280-880 nm)

The spectral reflection profiles for DP, LP and W coated discs in the spectral range of 280-880 nm are presented in Figure 2a-c. DP (dark pink) coated disc-surface display on an average 80% reflection in the spectral span 630-880 nm; the reflection significantly decreases between 630 and 560 nm, a small increase is registered in the span 560-415 nm. The reflection was lowest in the wavelength span lower than 400 nm (Figure 2a); at 550 nm for DP coated surface the reflectance of 10% was recorded. The mean reflectance in the spectral range 280-880 nm for DP was estimated as 44%. The reflectance profile for Light Pink (LP) coated surface was similar to that displayed by DP coated surface (Figure 2b), but the reflection was much larger (90 – 95%) in the wavelength span 880-600 nm. The second reflection peak was at 430 nm (70%) and the spread of the second peak was also larger. The lowest reflectance of around 10% was recorded in the span 280-380 nm. The mean reflectance in the spectral range 280-880 nm for light pink was 61%

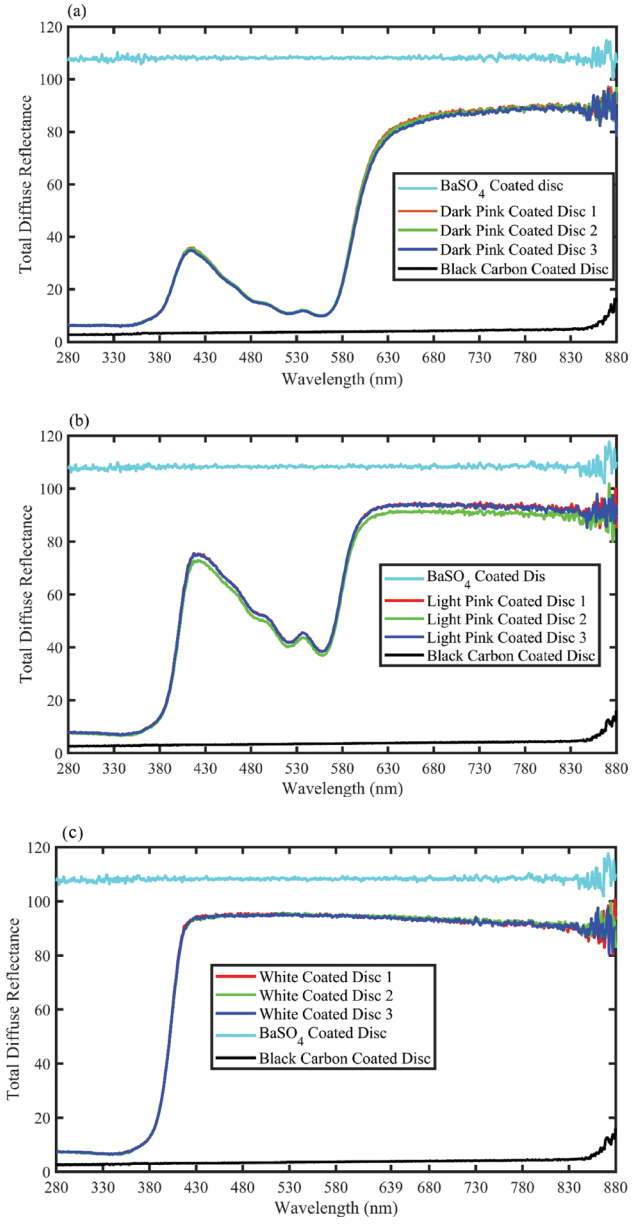

Figure 2: (a) Reflection profiles of three different discs coated with Dark Pink (DP) on cement surface (red, green and blue curves). Upper curve correspond to the perfectly reflecting surface (BaSO4; yellow colour) coated discs and the lower most curve is the profile of perfect absorber surface (black carbon coated discs; black colour). (b and c) represents the same for LP and W coated discs respectively.

The reflectance profile for white (W) colour coated discs is shown in Figure 2c; the surface reflected most of the radiation in the tested wavelength span (around 90%) in the spectral region 430-880 nm. However, the reflection profile below 380 nm was very low but still higher than DP and LP coated surfaces. The mean reflectance in the spectral range 280-880 nm for W coated surface was estimated as 76%. The extent of reflection was highest for W and lowest for the DP coated surface. It is important to state that in the wavelength span of visible light (400-700 nm) the averaged reflectivity respectively (W, LP and DP) was estimated as 90, 60 and 40% respectively. For the tested infrared range (701 to 880 nm), the average reflectivity for these surfaces was 90, 80 and 80%.

Transforming Reflection Profiles into Transformation Matrix to Determine the Extent of Reflection of SSW from the Surfaces

The obtained reflection profiles for three colour coated discs were normalized into fractional reflection values by dividing the whole profile with the average reflection profile obtained from $BaSO_4$ coated discs. The transformed reflection profiles provide fractional values ranging in the interval 0 (complete absorption) and 1 (complete reflection) (Figure 3). The obtained transformed values, now, could be analyzed to obtain the amount of solar radiation reflected if the roof surface is coated with these colours (W, LP, and DP). The reflectance was lowest for DP and highest for W coated surface. The fraction of incident solar radiation, integrated energy in the spectral span 280-880 nm from respective colour coats on surface W, LP and DP) was calculated as 76% (Figure 4a), 61% (Figure

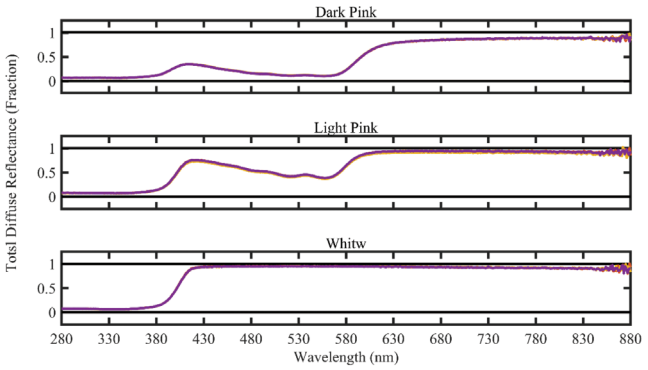

Figure 3: Fractional reflection profiles of DP, LP and W coated discs.

4b) and 44% (Figure 4c). It can be inferred that the colour of a surface has a direct bearing on the extent of reflection of incident SSW radiation, and this will also determine the amount of absorption at the surface and the surface temperature. Less SSW absorption will reduce the surface temperature: high reflectance has an important repercussion on the surrounding atmosphere's temperature.

As discussed earlier, the atmosphere is transparent to solar radiations confined within the visible spectral region. Consequently, if the fraction of radiation falling on a surface is reflected back, it will still be in the form of visible radiation, while the fraction of radiation not reflected will be absorbed and increase the temperature of the surface. The transformation of visible radiation (absorbed fraction) into heat will cause the heated surface to re-radiate the radiation back into space but as IR radiation. IR radiations can be absorbed by the GHGs present in the atmosphere, which will warm the atmosphere. The argument follows that if an absorbed fraction of the visible solar radiation can be reduced by altering the surface reflectance then the surface temperature will be low. The magnitude of the reflected IR radiation will also be low, which will have direct implications for the ambient environment's temperature.

Determining the Decrease in Temperature on the Surface Coated with DP, LP and W Colour Superseal Thermoflex P-111 coats

Following the quantitative estimates of the reflection profile in wavelength (280-880 nm) span for different colour coated surfaces, the extent of temperature decrease by these surfaces can be calculated. These calculations involve the average solar radiation incident on a surface by considering extraterrestrial solar energy spectral profile in the 280-880 nm range (Figure 1a,b). The actual values received on the ground, of course,

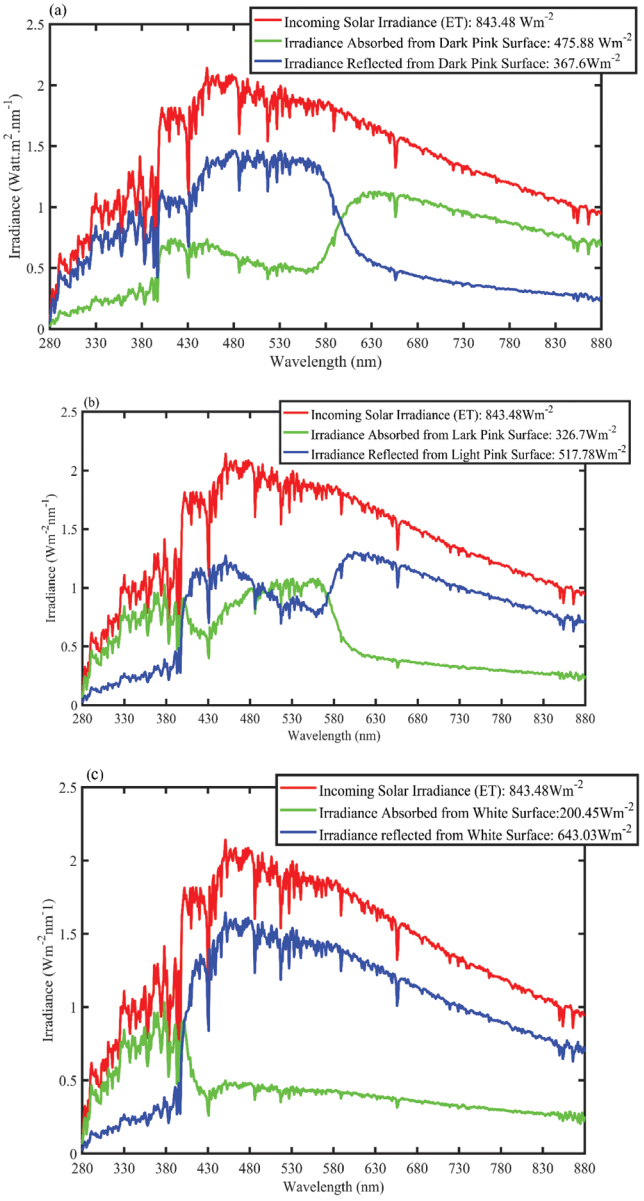

Figure 4: (a) Average extra-terrestrial solar radiation ($Wm^{-2}nm^{-1}$; red curve), the estimated reflected fraction determined on the basis of reflection profile shown by DP coated discs (blue curve) and the difference represents the amount absorbed by the surface (green curve). (b and c) represents the same for LP and W coated discs respectively.

will depend upon latitude, solar zenith angle, and the distance of the Sun from the Earth, at a particular time on a particular day of the year, etc. However, representative calculations can be done on the realistic values of the solar radiation by considering these factors, or by doing the actual measurement at a location using a spectral radiometer. In the present experiment, the data from the measured reflectance values from three

different colour coated surfaces enabled the calculations for the extent of absorbed solar radiation fraction at these surfaces. Knowing the absorbed energy fraction by the respective colour coated surfaces (DP, LP and W) further enabled the determination of surface temperature by using the Stefan-Boltzmann law. The calculated surface temperature for the respective coloured surfaces was 29 ^{o}C (DP), -2^{o}C (LP), and -30^{o}C (W) for DP, LP and W, respectively as given in the Table 2. These numbers are startling, however, they should be looked at by considering that these surfaces are exposed to the ambient environment and the actual temperature of these surfaces will change after taking into account the temperature of the surrounding atmosphere where greenhouse gases are present (Arnell et al., 2016; Arnfield, 2003). The calculations done in the present case assume ideal reflectance from the colour coated surfaces, in real situations the reflectance can be (a) diffuse, (b) specular and (c) diffuse anisotropic reflectance; the latter is more relevant in the present case. In general, the loss of energy in diffused reflectance is less than that from specular reflectance. This implies that the magnitude of absorbed energy over these surfaces may be a little higher than that calculated.

Table 2: Reflected, absorbed energy and temperature over DP, LP and W coated surface

Colour of the surface	*Reflected Energy (W/m^2)*	*Absorbed Energy (W/m^2)*	*Temperature (°C)*
DP	367..6	475.88	29
LP	517.78	326.7	-2
W	643.03	200.45	-30

To ascertain the temperature of a surface under a real condition, the whole roof surface of a house at Jawaharlal Nehru University was coated with W heat reflecting Superseal Thermoflex P-111 procured from Supertech Chemicals Specialties Pvt. Ltd. (Navi Mumbai, India). The roof surface of the adjoining house represented a dark asphalt coat, typically used for coating the roofs, as a reference. The experiment was done to measure the roof surface temperature by using non-contact Infrared thermometer equipped with a built-in laser pointer capable of measuring the surface temperature with ±0.1^{o}C from a distance (MEXTECH 8858/8859 series IR Thermometer, Mextech technologies India). The measurements were done on the 15th of May 2012 at 13:30 hrs Indian Standard Time (IST) under open sky conditions around solar-noon. The temperature recorded in the shade (under the white coated roof surface), 4 feet above the ground, was 41.8^{o}C; temperature recorded for the W coated roof surface, under the open sky and overhead sun was 34.6^{o}C; and temperature recorded for the reference asphalt roof surface was 58.8^{o}C. These measurements show that W coated roof surface will have a temperature significantly lower (-7.2^{o}C) than the ambient temperature, also the temperature difference between W coated roof surface and the asphalt roof surface was very significant (24.2^{o}C). Since the ambient atmosphere is in contact with the roof surface, its lower temperature should affect the ambient air's temperature too. In addition, a surface (roof) with higher reflectance or less absorbed energy will transfer (conduction) less heat below the surface. Therefore, the transfer of heat from the roof towards the room beneath will be significantly less. Consequently, the energy required to cool the room (air conditioning) will be reduced in comparison to the roof surface coated with an asphalt coating. The proposed strategy to cover the roof surfaces with a W coat in a large city will certainly contribute to lowering the ambient temperature: A surface area ≈70 km^2 can be used for the suggested strategy by appropriating 50% of the total available roof area in Delhi, the surface area large enough to make a difference (Attri, 2010; Zhang et al., 2020; Barnes et al., 2020; Wei et al., 2020)

Summary and Conclusions

The proposed strategy in this work is based on the physics of reflecting surfaces for SSW radiation which can be reflected efficiently back into space without getting trapped by the Earth's atmosphere. In this work, three colour (DP, LP, and W) coating samples were taken and reflectivity on the colour coated surfaces was measured in the available radiation range of 280 to 880 nm. It is observed that W coating reflects maximum and hence the temperature is lowest among the three colour coated surfaces. DP colour coated surface reflects less and the temperature over DP coated surface is maximum among the three colour coated surfaces. The approach is benign and can be easily applied on roof surfaces of the buildings and houses in large cities in hot tropical countries: a significantly large surface area can be appropriated for this. The absorption of SSW radiation on the appropriated roof surfaces would not only ensure significantly lower surface temperature but also low absorption. In addition to cooling the

surrounding ambient temperature, the surface will also emit much less IR radiation into the atmosphere for GWGs to trap. Any drop in the ambient temperature will in turn lower the energy required to cool the house/building interior spaces, thus lowering the fossil fuel consumption used in generating energy. Further experiments in this regard can fine-tune this approach's effectiveness by scaling up the experiment over a larger area in a city. The findings from this work can also be scaled up by similar studies done in different seasons.

Acknowledgement

Bikram Sen Sahu acknowledges Supertech Chemicals Specialties Pvt. Ltd. (Navi Mumbai, India) for providing Superseal Thermoflex P-111 as study material. PyariMohan Maharana acknowledges CSIR for providing a timely stipend (CSIR-RA).

References

Akbari, H., Menon, S. and Rosenfeld, A., 2008. Global cooling: Increasing world-wide urban albedos to offset CO_2. *Climate Change*, **94:** 275-286.

Allen, W.A., Gausman, H.W., Richardson, A.J. and Thomas, J.P., 1969. Interaction of isotropic light with a compact plant leaf. *Journal of the Optical Society of America*, **59:** 1376-1379.

Arnell, N.W., et al., 2016. The impacts of climate change across the globe: A multi-sectoralassessment. *Climatic Change*, **134:** 457-474.

Arnfield, A.J., 2003. Two decade of urban climate research: A review of turbulence, exchanges of energy and water, and the urban heat island. International *Journal of Climatology*, **23:** 1-26.

Attri, A.K., 2010. Can it be this easy?. The Times of India, Apr 6. www.indiaenvironmentportal.org.in/category/22536/author/arun-k-attri/)

Barnes, J.W., et al., 2020. Diffraction-limited Titan surface imaging from orbit using near-infrared atmospheric windows. *The Planetary Science Journal*, **1(1):** 24.

Bartos, M.D. and Chester, M.V., 2015. Impacts of climate change on electric power supply in the Western United States. *Nature Climate Change*, **5**: 748.

Ben-Dor, E. and Banin, A., 1995. Near-infrared analysis as a rapid method to simultaneously evaluate several soil properties. *Soil Science Society of America Journal*, **59:** 364-372.

Blonquist, J.M. and Bugbee, B., 2018. Solar, net, and photosynthetic radiation. Agroclimatology: Linking Agriculture to Climate, (agronmonogr60).

Bowyer, P. and Danson, F.M., 2004. Sensitivity of spectral reflectance to variation in live fuel moisture content at leaf and canopy level. *Remote Sensing of Environment*, **92:** 297-308.

Boyton, W.V., Sprague, A.L., Solomon, S.C., Starr, R.D., Evans, L.G., Feldman, W.C., Trombka, J.I. and Rhodes, E.A., 2007. Messenger and the chemistry of Mercury's surface. *Space Science Review*,. **131:** 85-104.

Brown, D.J., Shepherd, K.D., Walsh, M.G., Dewayne Mays, M. and Reinsch, T.G., 2006. Global soil characterization with VNIR diffuse reflectance spectroscopy. *Geoderma*, **132:** 273-290.

Caldeira, K. and Brown, P.T., 2019. Reduced emissions through climate damage to the economy. *Proceedings of the National Academy of Sciences*, **116(3):** 714-716.

Chen, J., Gao, C., Zeng, X., Xiong, M., Wang, Y. and Jing, C., et al., 2017. Assessing changes of river discharge under global warming of 1.5° C and 2° C in the upper reaches of the Yangtze River Basin: Approach by using multiple-GCMs and hydrological models. *Quaternary International*, **453:** 63-73.

Cui, Y., Mitomi, Y. and Takamura, T., 2009. An empirical anisotropy correction model for estimating land surface albedo for radiation budget studies. *Remote Sensing of Environment*, **113:** 24-39.

Denning, R.J., 2018. Camouflage fabrics. *In*: Engineering of High-Performance Textiles. 349-375.

Fischer, E.M. and Knutti, R., 2015. Anthropogenic contribution to global occurrence of heavy-precipitation and high-temperature extremes. *Nature Climate Change*, **5:** 560.

Gaffin, S.R., Imhoff, M., Rosenzweig, C., Khanbilwardi, R., Pasqualini, A., Kong, A.Y.Y., Grillo, D., Freed, A., Hillel, D. and Hartung, E. 2012. Bright is the new black-multiyear performance of high albedo roofs in urban climate. *Environmental Research Letters*, **7:** 014029 (12pp).

Goodin, D.G., Han, L., Fraser, R.N., Rundquist, D.C., Stebbins, W.A. and Sohallcs, J.F., 1993. Analysis of suspended solids in water using remotely sensed high resolution derivative spectra. Photogramm. *Engineering and Remote Sensing*, **59:** 505-510.

Henderson, T.L., Baumgardner, M.F., Franzmeier, D.P., Stott, D.E. and Coster, D.C., 1992. High dimensional reflectance analysis of soil organic matter. *Soil Science Society of America Journal*, **56:** 865-872.

Hossain, Md. M. and Min G., 2016. Radiative cooling: principles, progress, and potentials. *Advanced Science*, 3(7): 1500360.

Intergovernmental Panel on Climate Change. 2015. Climate change 2014: Mitigation of climate change (Vol. 3). Cambridge University Press.

Islam, K., Singh, B. and McBratney, A., 2003. Simultaneous estimation of several soil properties by ultra-violet, visible and near-infrared reflectance spectroscopy. *Australian Journal of Soil Research*, **41:** 1101-1114.

Jacobson, M.Z. and Ten Hoeved, J.E., 2012. Effects of urban surfaces and white roofs on global and regional climate. *Journal of Climate*, **25:** 1028-1044.

Jacquemoud, S. and Baret, F., 1990. PROSPECT: A model of leaf optical properties spectra. *Remote Sensing of Environment*, **34:** 75-91.

Jacquemoud, S., Bacour, C., Poilve, H. and Frangi, J.P., 2000. Comparison of four radiative transfer models to simulate plant canopies reflectance: Direct and inverse mode. *Remote Sensing of Environment*, **74:** 471-481.

Jacquemoud, S., Baret, F., Andrieu, B., Danson, F.M. and Jaggard, K., 1995. Extraction of vegetation biophysical parameters by inversion of the Prospect and sail models on sugar beet canopy reflectance data. Application to TM and AVIRIS sensors. *Remote Sensing of Environment*, **52:** 163-172.

Jacquemoud, S., Ustin, S.L., Verdebout, J., Schmuck, G., Andreoli, G. and Hosgood, B., 1996. Estimating leaf biochemistry using the PROSPECT leaf optical Properties model. *Remote Sensing of Environment*, **56:** 194-202.

Jahandideh-Tehrani, M., Haddad, O.B. and Loáiciga, H.A., 2015. Hydropower reservoir management under climate change: The Karoon reservoir system. *Water Resources Management*, **29:** 749-770.

James, R., Washington, R., Schleussner, C.F., Rogelj, J. and Conway, D., 2017. Characterizing half-a-degree difference: A review of methods for identifying regional climate responses to global warming targets. *Wiley Interdisciplinary Reviews: Climate Change*, **8:** 1-23.

Jin, Z., Charlock, T.P., Smith Jr., W.L. and Rutledge, K., 2004. A parameterization of ocean surface albedo. *Geophysical Research Letters*, **31(22)**. doi:10.1029/2004GL021180

Karmalkar, A.V. and Bradley, R.S., 2017. Consequences of global warming of 1.5 °C and 2 °C for regional temperature and precipitation changes in the contiguous United States. PloS one. 12, e0168697.

Kraaijenbrink, P.D.A., Bierkens, M.F.P., Lutz, A.F. and Immerzeel, W.W., 2017. Impact of a global temperature rise of 1.5 degrees Celsius on Asia's glaciers. *Nature*, **549:** 257.

Kraucunas, I., Clarke, L., Dirks, J., Hathaway, J., Hejazi, M. and Hibbard, K., 2015. Investigating the nexus of climate, energy, water, and land at decision-relevant scales: The Platform for Regional Integrated Modeling and Analysis (PRIMA). *Climatic Change*, **129:** 573-588.

Lakeman, J.A., 1996. Climate change 1995: The science of climate change: contribution of working group I to the second assessment report of the Intergovernmental Panel on Climate Change (Vol. 2). Cambridge University Press.

Levinson, R. and Akbari, H., 2002. Effects of composition and exposure on the solar reflectance of portland cement concrete. *Cement and Concrete Research*. **32:** 1679-1698.

Malthus, T.J. and Dekker, A.G., 1995. First derivative indices for the remote sensing of inland water quality using high spectral resolution reflectance. *Environment International*, 21, Ul-2X.

Marzo, A., Ferrada, P., Beiza, F., Besson, P., Alonso-Montesinos, J., Ballestrín, J., ... and Fuentealba, E., 2018. Standard or local solar spectrum? Implications for solar technologies studies in the Atacama desert. *Renewable Energy*, **127:** 871-882.

Matthews, E., 1983. Global vegetation and land use: new high resolution data bases for climate studies. *Journal of Climatology and Applied Meteorology*, **22:** 474487.

Mohammed, K., Islam, A.S., Islam, G.T., Alfieri, L., Bala, S.K. and Khan, M.J.U., 2017. Extreme flows and water availability of the Brahmaputra River under 1.5 and 2° C global warming scenarios. *Climatic Change*, **145:** 159-175.

Monteith, J.L., 1970. Solar radiation and productivity in tropical ecosystems. *Journal of Applied Ecology*, **9:** 747-766.

Mustard, J.F., Poulet, F., Gendrin, A., Bibring, J.P., Langevin, Y., Gondet, G., Mangold, N., Bellucci, G. and Altieri, F., 2005. Olivine and pyroxene diversity in the crust of Mars. *Science*, **307:** 1594-1597.

Myers, D.R., Emery, K. and Gueymard, C., 2004. Revising and validating spectral irradiance reference standards for photovoltaic performance evaluation. *Journal of Solar Energy Engineering*, **126(1):** 567-574.

Myrup, L.O., 1969. A numerical model of the urban heat island. *Journal of Applied Meteorology and Climatology,* **8(6):** 908-918.

Oke, Timothy R., 1982. The energetic basis of the urban heat island. *Quarterly Journal of the Royal Meteorological Society,* **108(455):** 1-24.

Pachauri, R.K., Allen, M.R., Barros, V.R., Broome, J., Cramer, W., Christ, R., et al., 2014. Climate change 2014: Synthesis report. Contribution of Working Groups I, II and III to the fifth assessment report of the Intergovernmental Panel on Climate Change (p. 151). IPCC.

Rayner, T., et al., 2019. Evaluating the adequacy of the outcome of COP21 in the context of the development of the broader international climate regime complex: deliverable 4.2; COP21-results and implications for pathways and policies for low emissions European societies.

Reference: Can it be this Easy? Arun K. Attri, The Times of India, Apr 6, 2010

Rizwan, A.M., Dennis, L.Y. and Chunho, L.I.U., 2008. A review on the generation, determination and mitigation of urban heat island. *Journal of Environmental Sciences,* **20(1):** 120-128.

Rosenfeld, A.H., Akbari, H., Rommm, J.J. and Pomerantz, M., 1998. Cool communities strategies for heat island mitigation and smog reduction, *Energy and Buildings*, **28:** 51- 62.

Sahu, B.S., Tandon A. and Attri A.K., 2017. Role of ozone depleting substances and solar activity in observed long-term trends in total ozone column over Indian region.

International Journal of Remote Sensing, **38:** 5091-5105. doi:10.1080/01431161.2017/1333654

Schleussner, C.F., Lissner, T.K., Fischer, E.M., Wohland, J., Perrette, M., Golly, A., et al., 2016. Differential climate impacts for policy-relevant limits to global warming: The case of 1.5 °C and 2 °C. *Earth System Dynamics*, **7:** 327-351.

Sellers, P.J., Mintz, Y., Sud, Y. C. and Dalcher, A., 1986. A simple biosphere model (SiB) for use within general circulation models. *Journal of Atmospheric Science*, **43:** 505-531.

Sellers, P., Los, S., Justice, C., Dazlich, D., Collatz, G. and Randall, D., 1996. A revised land surface parameterization (SiB-2) for atmospheric GCMs. Part 2: The generation of global fields of terrestrial biophysical parameters from satellite data. *Journal of Climate*, **9:** 706-737.

Shunlin, L, Alan, S. and Charles, W., 1998. Retrieval of land surface albedo from satellite observations: A simulation study. *Journal of Applied Meteorology*, **38:** 712-725.

Simposon, J.R. and Mcpherson, E.G., 1997. The effects of roof albedo modification on cooling loads of scale model residences in Tucson, Arizona. *Energy and Buildings*, **25:** 127-137.

Small, C., 2006. Comparative analysis of urban reflectance and surface temperature. *Remote Sensing of Environment*, **104:** 168-189.

Stoner, E.R. and Baumgardner, M.F., 1981. Characteristic variation in reflectance of surface soils. *Soil Science Society of American Journal*, **45:** 1161-1165.

Summers, D., Lewis, M., Ostendorf, B. and Chittleborough, D., 2011. Visible near-infrared reflectance spectroscopy as a predictive indicator of soil. Ecological Indicators. 11, 123-131. Doi:10.1016/j.ecolind.2009.05.001.

Tadeu, R., Prado, A. and Ferreira, F.L., 2005. Measurement of albedo and analysis of its influence the surface temperature of building roof materials. *Energy and Buildings*, **37:** 295-300.

UNFCCC, 2015. Decision 1/CP.21, The Paris Agreement. FCCC/CP/2015/10/Add.1

Ustin, S.L., Roberts, D.A., Pinzon, J., Jacquemoud, S., Gardner, M., Scheer, G., et al. 1998. Estimating canopy water content of chaparral shrubs using optical method. *Remote Sensing of Environment*, **65:** 280-291.

Van Vliet, M.T., Wiberg, D., Leduc, S. and Riahi, K., 2016. Power-generation system vulnerability and adaptation to changes in climate and water resources. *Nature Climate Change*, **6:** 375.

Vautard, R., Gobiet, A., Sobolowski, S., Kjellström, E., Stegehuis, A., Watkiss, P., et al., 2014. The European climate under a 2 °C global warming. *Environmental Research Letters*, **9:** 034006.

Viscarra Rossel, R.A., Walvoort, D.J.J., McBratney, A.B., Janik, L.J. and Skjemstad, J.O., 2006. Visible, near infrared, mid infrared or combined diffuse reflectance spectroscopy for simultaneous assessment of various soil properties. *Geoderma*, **131:** 59-75.

Weng, Q., Lu, D. and Schubring, J., 2004. Estimation of land surface temperature–vegetation abundance relationship for urban heat island studies. *Remote Sensing of Environment,* **89:** 467-483.

www.indiaenvironmentportal.org.in/category/22536/author/arun-k-attri/)

Xu, Y., Zhou, B.T., Wu, J., Han, Z.Y., Zhang, Y.X. and Wu, J., 2017. Asian climate change under 1.5–4° C warming targets. *Advances in Climate Change Research*, **8:** 99-107.

Wei, G., et al., 2020. Thermal-responsive PNIPAm-acrylic/Ag NRs hybrid hydrogel with atmospheric window full-wavelength thermal management for smart windows. *Solar Energy Materials and Solar Cells,* **206(1):** 10336.

Zhang, J., et al., 2020. Thin-film perfect infrared absorbers over single-and dual-band atmospheric windows. *Optics Letters,* **45(10):** 2800-2803.